

**HIGH RESOLUTION X-RAY FLUORESCENCE MICRO-TOMOGRAPHY  
ON SINGLE SEDIMENT PARTICLES**

L. Vincze, B. Vekemans  
Micro and Trace Analysis Center (MITAC)  
University of Antwerp, Belgium

I. Szalóki  
University of Debrecen, Hungary

K. Janssens, R. Van Grieken  
Micro and Trace Analysis Center (MITAC)  
University of Antwerp, Belgium

H. Feng, K. W. Jones  
Brookhaven National Laboratory  
Upton, New York USA

F. Adams  
Micro and Trace Analysis Center (MITAC)  
University of Antwerp, Belgium

Presented at

46th Annual Meeting of the SPIE (International Society for Optical Engineering)

International Symposium on Optical Science and Technology

San Diego, California

29 July - 3 August 2001

# High resolution X-ray fluorescence micro-tomography on single sediment particles

L. Vincze<sup>1</sup>, B. Vekemans<sup>1</sup>, I. Szalóki<sup>2</sup>, K. Janssens<sup>1</sup>, R. Van Grieken<sup>1</sup>, H. Feng<sup>3</sup>, K.W. Jones<sup>3</sup>, F. Adams<sup>1</sup>

<sup>1</sup>Micro and Trace Analysis Center (MITAC), University of Antwerp, Belgium

<sup>2</sup>University of Debrecen, Hungary

<sup>3</sup>National Synchrotron Light Source (NSLS), BNL, Upton, NY, USA

## ABSTRACT

This work focuses on the investigation of the distribution of contaminants in individual sediment particles from the New York/New Jersey Harbor. Knowledge of the spatial distribution of the contaminants within the particles is needed to enable (1) more sophisticated approaches to the understanding of the fate and transport of the contaminants in the environment and (2) more refined methods for cleaning the sediments.

The size of the investigated particles ranges from 30-80 microns. Due to the low concentration of the elements of interest and the microscopic size of the environmental particles in these measurements, the small size and high intensity of the analyzing X-ray beam was critical. The high photon flux at the ESRF Microfocus beam line (ID13) was used as the basis for fluorescence tomography to investigate whether the inorganic compounds are taken upon the surface organic coating or whether they are distributed through the volume of the grains being analyzed. The experiments were done using a 13 keV monochromatic beam of approximately 2  $\mu\text{m}$  in size having an intensity of  $10^{10}$  ph/s, allowing absolute detection limits on the 0.04-1 fg level for Ti, Cr, Mn, Fe, Ni, and Zn.

## 1. INTRODUCTION

The waters of the NY/NJ Harbor drain into the Atlantic Ocean through a complex marine and estuarine system. A complex interplay of the river currents with tidal effects moves sediments back and forth in the Harbor. Due to decreased water velocity in this area sediment particles have more time to settle to the bottom and the Harbor performs as a sediment trap. During this sediment transport these particles interact with contaminants. The contaminants in sediments are the result of decades of industrial and other anthropogenic activities, such as industrial outfalls, sewage treatment plants, urban runoff, leachate from adjacent landfills, atmospheric deposition, etc. Many pollutants attach (adsorb) to sediment particles. Sediments deposited from polluted waters have larger amounts of pollutants than sediments deposited earlier, before pollution began. At different places in the world monitoring programs has been set up and databases are being created in order to understand the distribution and mobility of sediment contaminants to support environmental management [1-6]. The sediments found in the NY/NJ Harbor are generally very fine-grained silts and clays ( $< 0.1$  mm particle size) with a small fraction of larger grain sizes and large-size debris, and contaminants mostly associate with these fine-grained sediments [6].

Considering an estimated volume of several millions cubic meters of dredged material per year the disposal of large amount of dredged material becomes very important in order to maintain the Harbor in operation. Sediment decontamination seems to be the only publicly accepted option, being the only solution that reduces or eliminates the toxic organic and inorganic compounds that may cause harmful environmental and human-health effects.

Recently, technologies were proposed in order to process dredged material from the Port of New York and New Jersey [6,7]. The sediment washing process proposed by BioGenesis employs mechanical scouring of the dredged material, performed by a high-pressure jet of water (collisions) with application of biodegradable surfactants (detergents), chelating agents, and oxidizing chemicals to clean the particle surfaces. Chelating chemicals are used to render metals soluble so that they are transferred from the solid to the surrounding liquid. In a next step, the contaminants that are removed from the dredged material are treated by producing bubbles that create a local region of high temperature that destroys the organic compounds in the water (cavitation-oxidation). Floatable organic material is separated by surface skimming in a flotation tank, and metals are precipitated in the form of a sludge which is disposed of at a landfill.

Knowledge of the grain size distribution of the contaminants throughout single sediment particles is needed to enable more sophisticated approaches to the understanding of the fate and transport of the contaminants in the environment and more refined methods for cleaning the sediments. In this work, the high X-ray photon flux at the ESRF was used as the basis for fluorescence tomography to investigate whether the inorganic compounds are taken upon the surface organic coating or whether they are distributed through the volume of grain being analyzed. Due to the low concentration of the elements of interest and the microscopic size of the environmental particles in these measurements, the small size and high intensity of the analyzing X-ray beam was critical.

## 2. EXPERIMENTAL

At the Microfocus beamline of the ESRF (ID13), shown schematically in Fig.1, tapered glass capillaries have routinely been used as add-on optics to produce an X-ray micro beam with sizes down to  $2\ \mu\text{m}$  and intensities over  $10^{10}$  ph/s at an energy of 13 keV within an energy bandwidth of  $\Delta E/E \approx 10^{-4}$  [8,9].

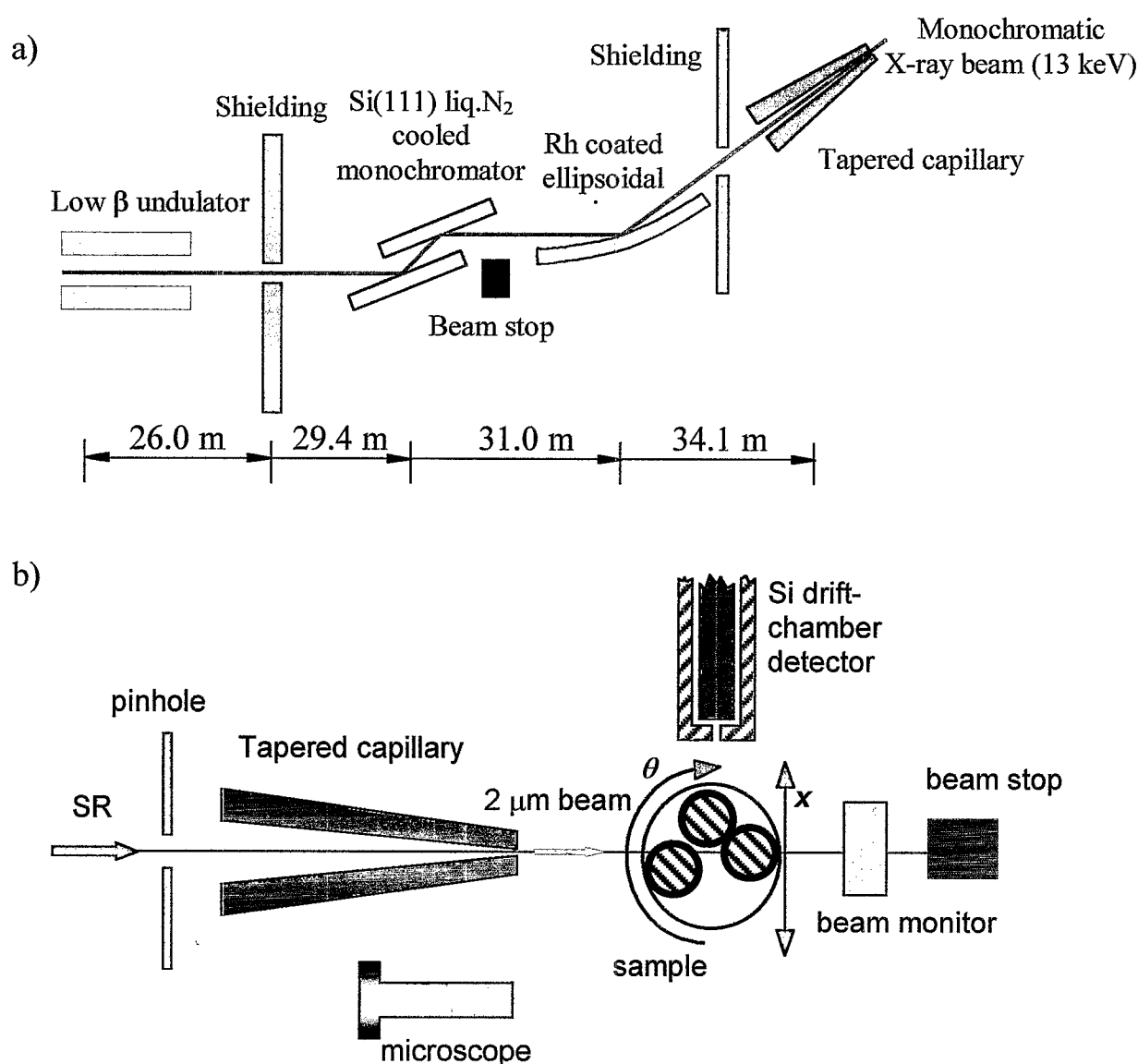


Fig.1 Schematic representation of the Microfocus beamline (ID13) of the ESRF where the experiment was performed (a) and the experimental arrangement for the XRF microtomography (b).

The primary X-ray source employed here is a low beta undulator with a source size of  $0.139 \times 0.026 \text{ mm}^2$  (HxV FWHM) and divergencies of  $0.233 \times 0.020 \text{ mrad}^2$  (HxV FWHM). The undulator beam, after monochromatization by a  $\text{LN}_2$ -cooled  $\text{Si}(111)$  channel-cut monochromator, is focused by a Rh coated ellipsoidal mirror located at a distance of 31 m from the source having a theoretical demagnification of 10. This mirror produces a photon beam with sizes of  $16 \times 27 \text{ }\mu\text{m}^2$  (HxV FWHM) and divergencies of  $2.4 \times 0.3 \text{ mrad}^2$  (HxV FWHM) with an overall intensity of about  $10^{13} \text{ ph/s}$  at 13 keV. The focused photon beam is further concentrated down to the  $2 \text{ }\mu\text{m}$  level using a tapered glass capillary. The capillary optic at this energy produces a slightly divergent beam of about  $1 \text{ mrad}^2$ . The set-up allows absolute detection limits on the 0.04-1 fg level in 1000 s live time for Pb, Cr, Fe, Zn and As, as shown in Fig.2.

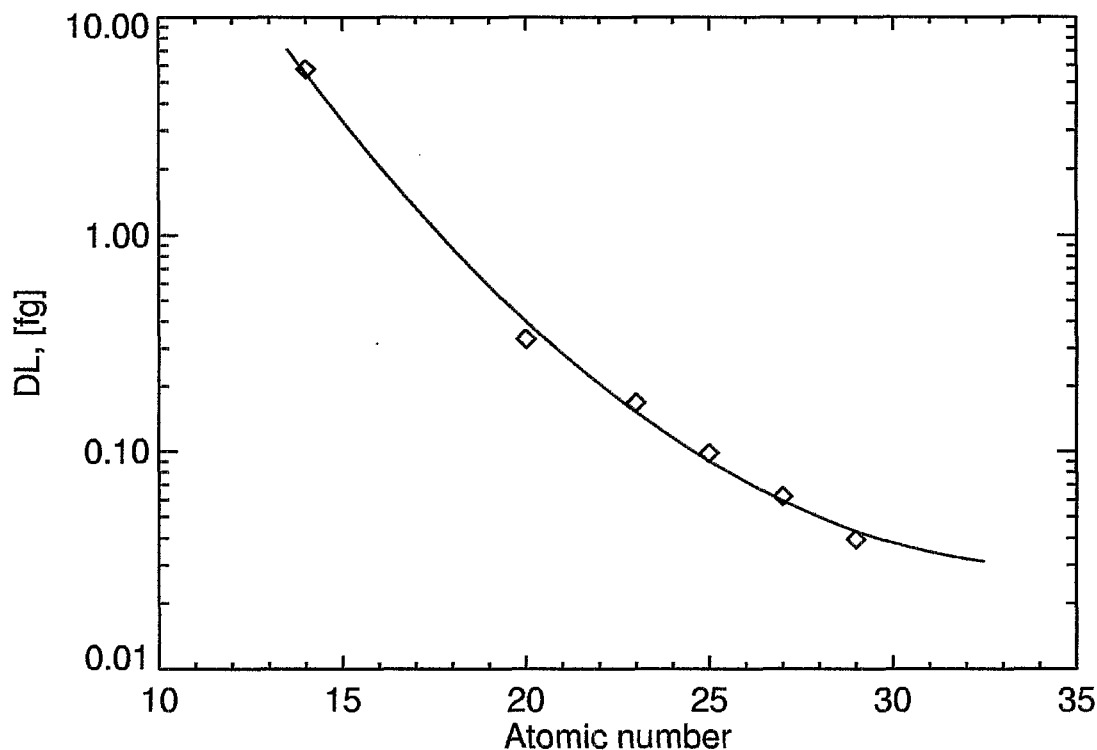


Fig.2 Absolute detection limits measured in 1000 s live time at the set-up shown in Fig.1. The above detection limits were determined using the standard reference material NIST SRM 1832 (thin glass calibration standard).

The XRF tomography was performed by repetitive horizontal scans through the micro beam using a particle dependent step size in the range of  $1.6 - 4 \text{ }\mu\text{m}$  within the angular interval of  $0$  to  $180^\circ$ . The angular increment was typically  $3^\circ$ . A tomographic scan typically consisted of 60 translational and 60 rotational steps with a live time of 1-8 s per point. Next to the analysis of sediment particles of the NY/NJ Harbor, for comparison, several sediment particles sampled from the North Sea (Dutch coastal area) were also put under investigation. Table 1 summarizes the origin and the various cleaning treatments of the investigated particles prior to the experiment. The particles were mounted on glass capillary fibers of  $100 \text{ }\mu\text{m}$  in diameter using so-called rubbercement glue. Fig.3 shows scanning electron microscope images of two mounted particles, originating from the North Sea and New York harbor, respectively. Table 2 shows their (low atomic number) major composition determined by electron probe micro analysis (EPMA) by taking the average of analytical results corresponding to 20 distinct points on each particles. The quantitative data were obtained by so-called reverse Monte Carlo quantification, developed specifically for EPMA measurements.



Fig.3 Scanning electron microscope images of sediment particles mounted on glass capillary fibers to perform the XRF micro-tomography. Left panel: sediment particle from New York Harbor and right panel: sediment particle from the North Sea (Dutch coast area).

Particle	Origin	Preparation
NY1-1	Stratus Petroleum (Newark Bay)	Untreated
NY2-1	Stratus Petroleum (Newark Bay)	Untreated
NY9-1	Stratus Petroleum (Newark Bay)	Washed
4159	North Sea (Dutch Coastal Area)	Ultrasonic
4231-2	North Sea (Dutch Coastal Area)	Ultrasonic

Table 1. Names, origin and treatment of the examined sediment particles. Here “washed” refers to mechanical scouring by a high-pressure jet of water with application of surfactants, chelating agents and oxidizing chemicals and “ultrasonic” refers to ultrasonic treatment in distilled water.

Element	Concentration (%)	Concentration (%)
C	5.3	9.5
N	2.2	2.2
O	47.8	41.1
Na	4.0	0.5
Mg	1.0	1.0
Al	10.6	22.2
Si	27.1	19.1
S	0.04	0.06
Cl	0.01	0.2
K	1.1	4.3
Ca	1.3	0.15

Table 2. Major element composition of the particles shown in Fig.3 as determined by electron probe micro analysis (EPMA).

### 3. RECONSTRUCTION METHOD

The data obtained from a conventional translational or linear scan on a sample can be considered as a one-dimensional projection of the compositional structure of the irradiated slice of the sample (Fig. 4a). By means of many one-dimensional projections of the slice under different observation angles it is possible to reconstruct two-dimensional information (tomograms) on the elements in the slice of interest (Fig. 4b). The reconstruction technique applied in this work is generally known as Back-Projection [10] and is based on the RIEMANN procedure [11].

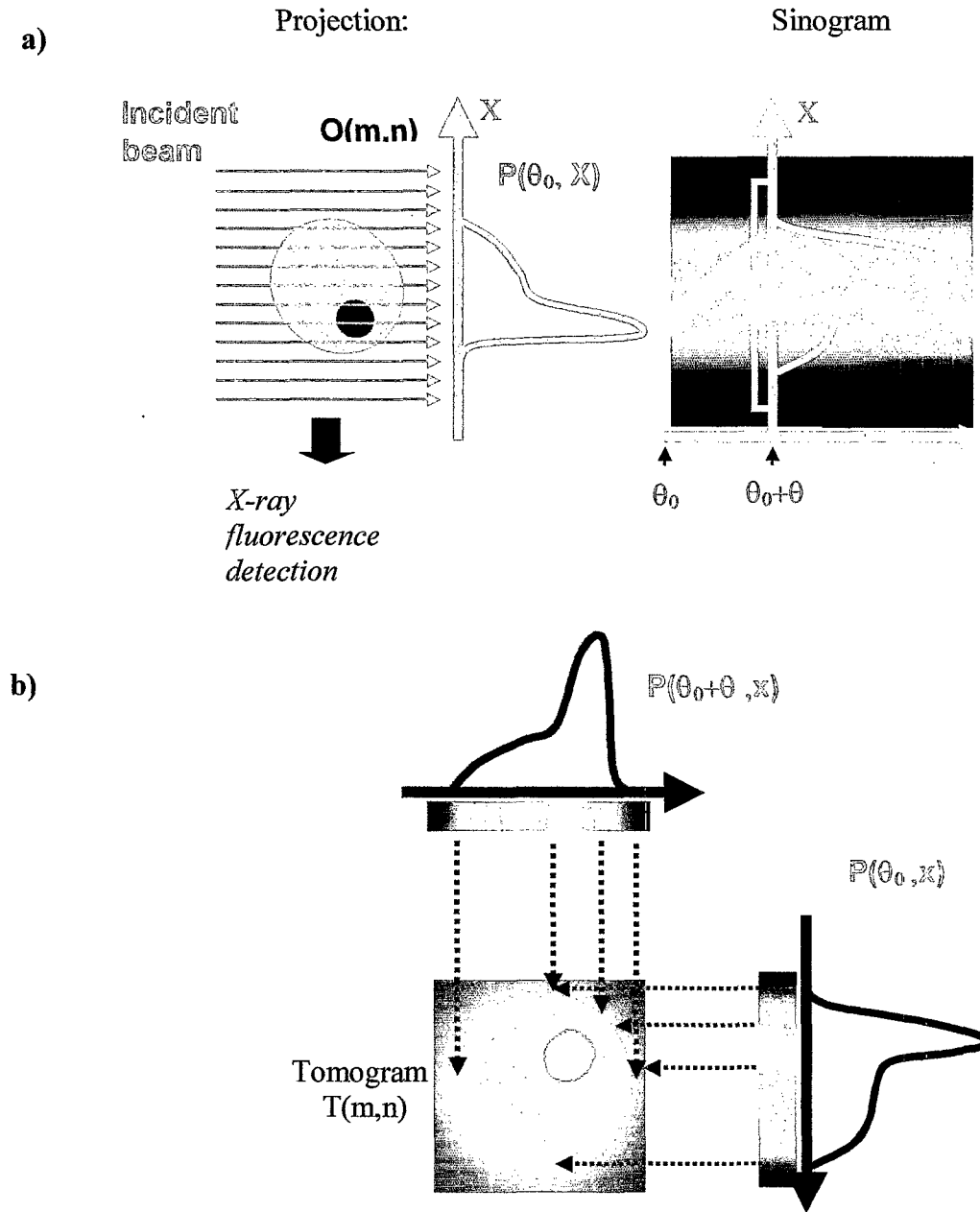


Fig. 4 An XRF sinogram  $S$  consists of one-dimensional projections corresponding to the variation of the detected fluorescence signal as the sample scanned (a). In practice linear scans are performed throughout the sample  $O$  under many observation angles  $\theta$ . Principle of backprojection (b).

Given the slice  $T(m,n)$ , which will contain the reconstructed slice (tomogram), each projection  $S(x, \theta)$  is "back-projected" into  $T$  taking into account the angle  $\theta$  at which the projection was performed experimentally (see Fig. 4b.). For each element of  $T$ , the values of the closest elements of the back-projected projections  $S(x, \theta)$  are then summed and stored in  $T$ . The appearance of star-like artifacts around 'hot-spots', an inherent characteristic of the back-projection process, is suppressed by the application of a filter, i.e. convolution of the one-dimensional projection data, prior to the actual back-projection.

#### 4. RESULTS AND DISCUSSION

Fig.5a shows typical sinograms and the corresponding reconstructed elemental distributions in the investigated slice obtained from particle NY9-1, a cleaned particle from NY Harbor. A translational step-size of  $3 \mu\text{m}$  was used, slightly larger than the beam size. While the sinograms suggest the presence of several hot-spots of K, Fe and Zn, in the reconstructed elemental maps these micron-sized areas of elevated K, Fe and Zn concentrations are less separated, appearing quite homogeneously distributed within the entire examined particle cross-section.

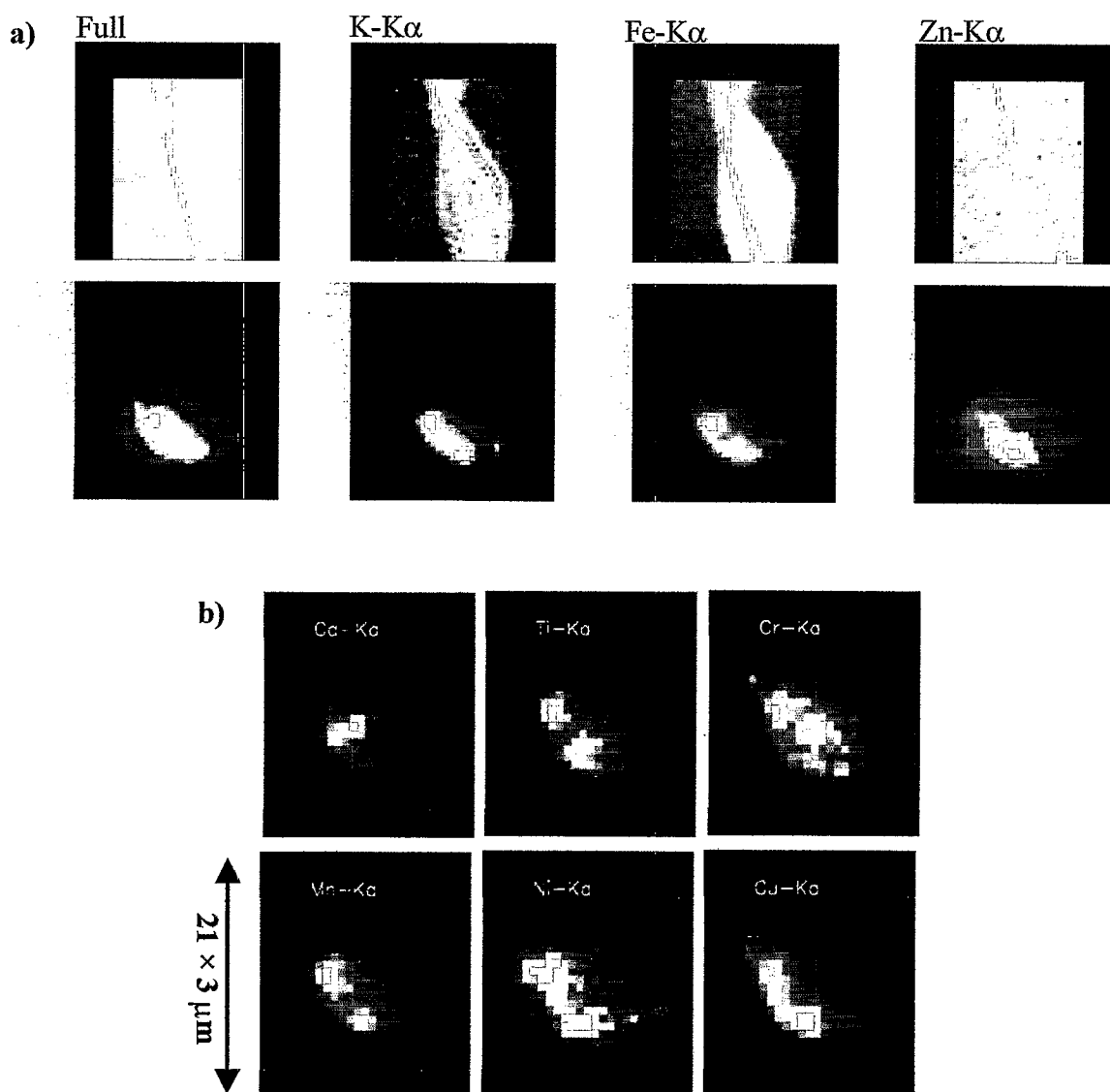


Fig.5 Measured elemental sinograms and reconstructed elemental maps from particle NY9-1 for the integrated spectral intensity as well as K, Fe and Zn (a). Reconstructed elemental maps corresponding to Ca, Ti, Cr, Mn, Ni and Cu (b).

The loss in resolution can be attributed to the relatively small number of projections used in these scans. Fig.5b shows the reconstructed maps of the remaining elements detectable in this particle, from which it is clear that contaminating metals such as Cr, Ni, Cu, and Zn are present throughout the entire sample cross-section, rather than being concentrated on the surface layer. This is probably the result of the applied decontamination process, which removed the surface organic coating layer together with the attached inorganic constituents.

Fig.6 shows the reconstructed elemental maps for two untreated sediment particles from the same area, called NY1-1 and NY2-1. In both cases, the metal constituents (Cr, Mn, Fe, Ni, Cu, Zn) are located within the surface layer, clearly forming small, 1-5  $\mu\text{m}$  sized, areas of high concentration. Elemental distributions corresponding to the particle matrix elements, such as K and Ca, define the shape of the particle cross-section. The reconstruction of these elemental maps suffer from significant sample self-absorption due to the low energies of their characteristic lines.

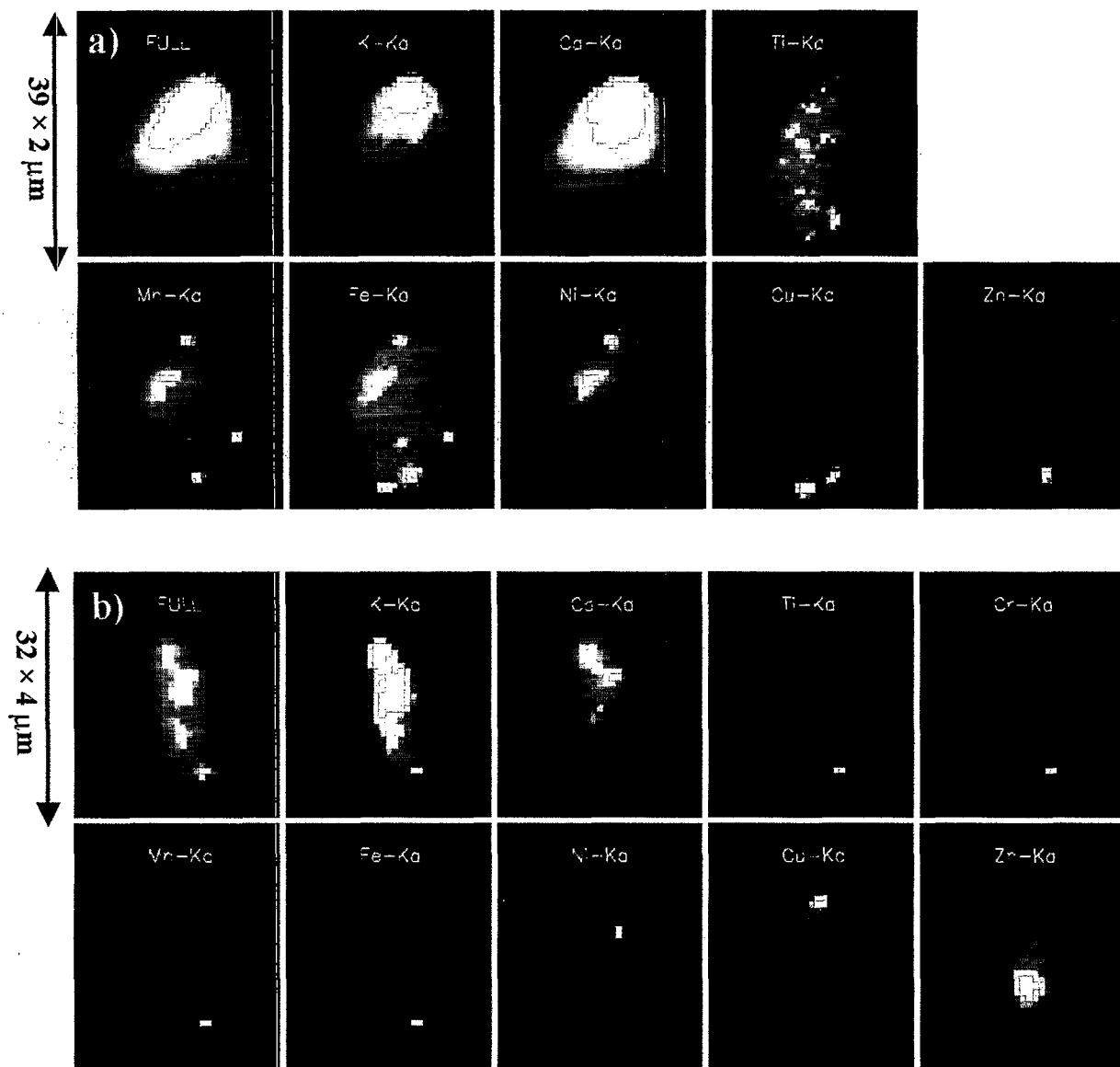


Fig.6. Reconstructed elemental maps from particle (a) NY1-1 and (b) NY2-1.



As comparison, two series of reconstructed elemental distributions are shown in Fig.7 corresponding to sediment particles sampled from the North Sea (Dutch coastal area). These particles were cleaned by ultrasonic treatment in distilled water. Pixel size of 1.6  $\mu\text{m}$  was used in case of particle #4159 and 2.2  $\mu\text{m}$  in case of particle #4231-2. Again, the detectable matrix elements K and Ca as well as the integrated spectral intensity distribution (denoted as "FULL") reveal the rather regular, quasi-circular cross-section of these sediment particles. Heavier elements, such as Cr, Mn, Fe and Zn are found to form shell-like structures near the particle surface area in case of particle #4159 while Ti, Ni and Cu are concentrated in small areas. The presence of hot-spots of Ti, Cr, Fe, Ni, Cu and Zn located close to the particle surface is characteristic to the second investigated North Sea sediment particle. A notable exception is Mn which is uniformly distributed in the examined slice.

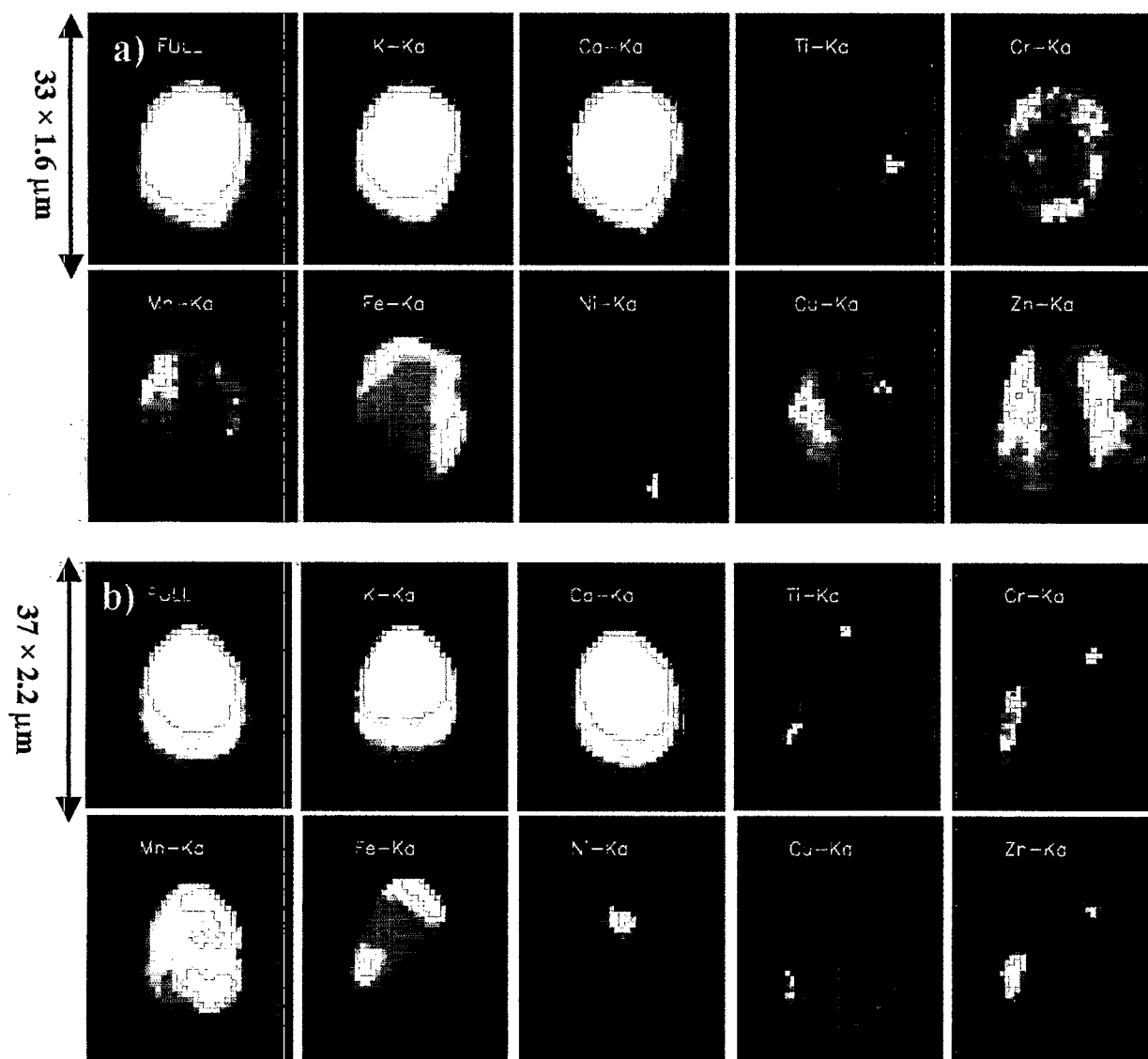


Fig. 7 Reconstructed elemental maps from particle (a) 4159 and (b) 4231-2.

## 5. CONCLUSIONS

X-ray fluorescence micro-tomography on single sediment particles in the size range of 30-80  $\mu\text{m}$  is demonstrated down to a resolution level of 2  $\mu\text{m}$ . The small beam size and high X-ray intensity allowed to perform these measurements with fg level absolute detection limits which was sufficient to detect heavy metal contaminants of low concentration, in many cases down to trace concentration levels.

The investigated untreated particles from NY/NJ harbor show elevated levels of transition metal contaminants, such as Cr, Fe, Ni, Cu, Zn to be located in micron sized hot-spots on the sample surface. Similar trend can be observed in case of the control sediments from the North-Sea Dutch coastal area: the particles show most of the contaminating metals near the surface layers of the particles. The cleaned particles from NY harbor, on the other hand, show no surface contamination indicating the effectiveness of the decontamination process. In this case, residual contamination, distributed within the entire examined particle cross-section has been found.

## ACKNOWLEDGEMENTS

L. Vincze is a fellow of the Belgian National Science Fund (FWO). Work supported in part by the US Department of Energy under contract number DE-AC02-98CH10886 (HF and KWJ). The authors acknowledge the help and support of C. Riekel and A. Simionovici throughout the work.

## REFERENCES

- [1] E. Mecray, M. ten Brink and B. Butman; U.S. Geological Survey, Fact Sheet 99-114, 1999.
- [2] F. Manheim, M. ten Brink, P. Hastings and E. Mecray; Contaminated-Sediment Database Development and Assessment in Boston Harbor; U.S. Geological Survey, Fact Sheet FS-078-99, 1999.
- [3] E. Mecray and M. ten Brink; Contaminant Distribution and Accumulation in Sediments of Long Island Sound: Initial Results; Fact Sheet FS-113-99, U.S. Geological Survey, 1999.
- [4] D. Walker, G. Passfield, S. Phillips; Stormwater Sediment Properties and Land Use in Tea Tree Gully, South Australia; AWWA 17<sup>th</sup> Federal Convention, Proceedings, Vol.2.
- [5] Baltic Sea Environment Proceedings, 27 A-D, 1979.
- [6] E. A. Stern, H. Feng and K. W. Jones; Source, Transport and Environmental Ecological Effect of Contaminated Sediments in the NY/NJ Harbor; Society of Environmental Toxicology and Chemistry (SETAC) 20<sup>th</sup> Annual Meeting, 1999.
- [7] K. W. Jones, E. A. Stern, K. R. Donato, and N. L. Clesceri; Sediment decontamination treatment train: commercial-scale demonstration fo the port of New/New Jersey; Proceedings Nineteenth Western Dredging Association (WEDA XIX) Annual Meeting and Conference and Thirty-first Texas A&M University Dredging Seminar; Louisville, Kentucky, 1999.
- [8] P. Engström, C. Riekel, C.H. Chanzy, ESRF Newsletter (1995).
- [9] P. Engström, C. Riekel, J. Synchr. Rad., 3, 97 (1996).
- [10] J. C. Russ; The Image Processing Handbook, 2<sup>nd</sup> ed.; CRC Press, Boca Raton, 1994.
- [11] S. Park and R. Schowengerdt; Image Reconstruction by Parametric Cubic Convolution; Computer Vision, Graphics & Image processing, 23, 256 (1983).